Egyptian Journal of Chemistry

http://ejchem.journals.ekb.eg/

Equilibrium Kinetic and Thermodynamics Studies of Uranium Adsorption by Natural Clinoptilolite from an Acidic Medium

Hager Nasser El Shamy[1], Mostafa Khalil[1], Mohamed Shaaban Atrees[2], El Sayed Ali Haggag[2], Mohamed Ismaiel Mahmoud El Aoady [2], Amira Mohamed Tawfik [2] and Hend Abdelkhalik Salem[2]

(1) Department Chemistry, Faculty of Science - Ain Shams University
(2) Nuclear Materials Authority, P.O. Box 530, El Maadi, Cairo, Egypt

Abstract

The equilibrium and kinetic characteristics of the natural clinoptilolite from an acidic medium have been determined. The adsorption parameters including pH, contact time, stirring rate, and temperature have been optimized. The practical adsorption capacity of uranium upon the resin under the optimum conditions has been found to attain 32 mg/g which matches with Langmuir isotherm 34.25 mg/g. The physical parameters including the adsorption kinetics, the isotherm models, and the thermodynamic data have also been determined to describe the nature of the uranium adsorption by the natural clinoptilolite. The working natural clinoptilolite was found to agree with both the pseudo-second-order reaction and the Langmuir isotherm. Scanning electron microscope (SEM), X-ray diffraction (XRD), and Thermogravimetric analysis (TGA) were used to examine the structure of the resulting adsorbent.

***Keywords*:** Natural clinoptilolite, uranium adsorption, kinetics, thermodynamics

I. Introduction

Zeolites are hydrated aluminosilicates of alkaline and alkaline-earth metals. About 40 natural zeolites have been identified during the past 200 years; the most common are analcime, chabazite, clinoptilolite, erionite, ferrierite, heulandite, laumontite, mordenite, and phillipsite. More than 150 zeolites have been synthesized; the most common are zeolites A, X, Y, and ZMS-5; Natural and synthetic zeolites are used commercially because of their unique adsorption, ion-exchange, molecular sieve, and catalytic properties. Major markets for natural zeolites are pet litter, animal feed, horticultural applications (soil conditioners and growth media), and wastewater treatment. Major use categories for synthetic zeolites are catalysts, detergents, molecular sieves [1-3].

Clinoptilolite series minerals are the most common zeolites in nature and have been found in many areas all around the world, for instance, in Europe (Hungary, Italy, Romania, Slovakia, Slovenia, Turkey, former Yugoslavia), in Russia, and several states of the former Soviet Union (Georgia, Ukraine, Azerbaijan), Asia (China, Iran, Japan, Korea), Africa (South Africa), Australia and New Zealand, and in many countries of the Americas, such as Argentina, Cuba, Mexico and the United States[4-7]. Parent rocks commonly contain over 50% of clinoptilolite, but contents over 80% are very widespread too [8]. Clinoptilolite belongs to the group heulandite (HEU), which possesses a two-dimensional structure [9].

Uranium is one of the most important elements because of its strategic importance in the energy field [10]. The World Nuclear Association "WNA" reports that there are 439 nuclear reactors operable in 30 countries as of January 1, 2016. As of January 1, 2016, 66 nuclear reactors are under construction in 14 countries and about 224 reactors that be either under construction by 2030. Accordingly, the uranium demand could grow by over 48% to as high as 266.8 million pounds U_3O_8 by 2030 from an estimated 179.3 million pounds of U_3O_8 in 2015 [11, 12].

In general, several methods have been carried out for recovery of uranium from uranium leach liquors or effluents as ultrafiltration [13],nanofiltration [14], resin-in-pulp [15], liquid membrane [16], biosorption [17], liquid-liquid extraction [18], ion exchange [19],solid-phase extraction [20], co-precipitation [21] and electrodeposition [22]. Among

*Corresponding author e-mail: msatrees@yahoo.com.; (Mohamed Shaaban Atrees).
Receive Date: 27 September 2021, Revise Date: 14 December 2021, Accept Date: 21 December 2021
DOI: 10.21608/EJCHEM.2021.98150.4573

these methods, the ion exchange method employing synthetic resin has received considerable interest compared to others, which is due to its selectivity, less sludge volume, metal recovery at low concentrations from aqueous solution, and ability to regenerate the resin [23].

The present work is concerned with studying the uranium extraction from acidic solution by a batch technique using natural clinoptilolite and determining the equilibrium and kinetic characteristics as well as the interesting thermodynamic data of the natural clinoptilolite for uranium recovery from an acidic solution. To realize the objectives of this work, the various parameters of uranium (VI) adsorption upon the studied natural clinoptilolite have been experimentally optimized as a pre-requisite for the determination of the relevant physical characteristics.

II. Experimental

2. Materials and methods

2.1. Chemicals and reagents

All chemicals used for analysis were analytical-grade reagents. Uranyl sulfate trihydrate $UO_2SO_4.3H_2O$ from IBI labs, Florida, USA and HCl 37%, HNO_3, NaCl**.**

2.2. Analytical method

The concentration of uranium in the aqueous solution (Ceq, mg/L) was analyzed at 650 nm using Arsenazo III dye. (Shimadzu UV–VIS-1601-spectrophotometer).

2.3 Physical and Chemical Properties of natural clinoptilolite.

Table (1) shows the Physical properties of natural clinoptilolite. Table (2) shows the chemical composition of Natural Clinoptilolite as received by using ICP analysis.

Table (1): The Physical Properties of natural clinoptilolite

Bulk (Particle) Density,mcm^{-3}	1.83	Apparent (Skeletal) Density,mcm^{-3}	2.377
Overall Surface Area, m^2gm^{-1}	89.82	Appearance(Color)	Greyish-white
Porosity, %	27.80	Humidity,%	6.75
Total Pore Area,m^2gm^{-1}	35.836	L.O.I,%*	13.6
Average Pore Diameter,µm	0.0181	Hardness, Moh'no.	4
Solubility,%	7.38		
Swelling Index	2.52	Grain Size	6 mm<
pH	6.8		

Table (2): the chemical composition of Natural Clinoptiloliteusing ICP

Elements	**Si**	**Al**	**Fe**	**K**	**Ca**
Wt.%	**62.88**	**11.52**	**5.63**	**4.85**	**3.94**

2.4.Preparation of the pregnant solutions:

- Generally, the samples used in this work were weighed using an analytical balance produced by Shimadzu (AY 220).
- Hot plate magnetic stirrer model Fisher Scientific.
- The hydrogen ion concentration of the different solutions was measured accurately using the pH-meter model (HAANA pH-mV-temp).
- The quantitative analysis of uranium was carried out by UV-spectrophotometer "single beam multi-cells-positions model SP-8001", Metretech Inc., version 1.02using Arsenazo III indicator (Sigma-Aldrich) [24]and confirmed by an oxidimetric titration against ammonium metavanadate using N-phenyl anthranilic acid indicator (Sigma-Aldrich).

2.5. Experimental procedure:

The batch procedure was performed to optimize the basic equilibrium conditions for uranium adsorption such as pH, contact time, temperature, and natural clinoptilolite to liquid ratio. In these experiments, 50 ml of 50 mg U/L solution were stirred with 1.0 g dry natural clinoptilolite200 rpm in a 100 ml conical flask. After mixing the clinoptilolite with the liquor, the two phases were decanted and the clear raffinate was analyzed against the uranium concentration. The amount of uranium adsorption QE (mg/g) was calculated from the difference of uranium concentration in the aqueous solution before and after adsorption at the equilibrium time t according to equation (1):

$$q_e = (C_0 - C_e)\frac{V}{m} \quad \textbf{(1)}$$

Where Co and Ce are the initial and equilibrium concentrations of U (VI) in the solution (mol. L-1), V is the volume of solution (L), m is the weight of the clinoptilolite(g). The amount of U (VI) adsorbed onto the resin (q, mg/g) and the uptake percent (U %) were determined using equation (2).

$$\boldsymbol{U\ \%} = \frac{(C_0 - C_e)}{C_e} \times 100 \quad \textbf{(2)}$$

The distribution coefficient (K_d) of uranium between the aqueous bulk phase and the solid phase clinoptilolite was calculated from the following equation (3):

$$K_d = \frac{C_o - C_e}{C_e} \times \frac{V}{m} \quad (3)$$

3. Results and Discussion

3.1. Characterization of the Clinoptilolite

3.1.1Mineral component of clinoptilolite

The attached XRD pattern of the sample confirms its Clinopitolite mineralogy by using X-ray Diffraction analysis which was applied to detect the crystallinity of the extracted samples of chitin and their corresponding clinoptilolite. A Scanting powder diffractometer was used for this purpose between 2θ angles of 5o and 40o. Ni-filtered Cu Kα -radiation was used as the X-ray source. The relative crystallinity of the polymers was calculated by dividing the area of the crystalline peaks by the total area under the curve as shown in Figure (1).

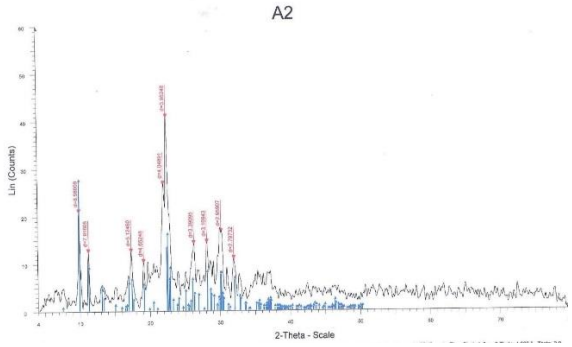

Figure (1): XRD patterns of Clinopitolitebefore uranium adsorption

3.1.2.Surface Morphology Studies

The SEM photographs in Fig.2 were taken at 100magnifications to observe the surface morphology of clinoptilolite. SEM micrographs of clinoptilolite display that the clinoptilolite has a drusy texture with very high microporosity, partially developed crystalline laminar habits, and conglomerates of compact crystals. Some small amorphous particles surrounding the crystal clusters can be seen in the SEM image.SEM analysis after adsorption confirms the presence of uranium on the clinoptilolite sorbent. After uranium ion sorption the efficient binding of the metal is characterized by the appearance of well-resolved uranium signals. The microscopic observation of the surface of sorbent particles after uranium ion sorption does not show significant changes in the external structure [25, 26].

3.1.3.Thermal analysis

Thermogravimetric analysis is a tool to investigate thermal Stability of Materials, oxidative decomposition, and vaporization of the clinoptilolite. Thermal decomposition behavior of the clinoptilolite related to the chemical composition and chemical bonding in the material structure is essentially determining the shape of the TGA-DTA profile. The thermal decomposition of clinoptilolite is mainly divided into three stages, each with elevated temperatures as shown in **Figure (3).** The first stage shows weight loss at 26.9-236°C corresponds to residual water evaporation. The second stage is between 236 and 558°C shows weight loss may be due to the fracture and digestion of clinoptilolite. The third stage is due to the degradation of clinoptilolite at 548–703°C. There is no change in weight loss over 700 °C. On the other hand, the DTG graph plot approves the breakdown of the sample and signifies the precise temperature at which the breakdown starts and ends. The deterioration because of the loss of water starts at 27℃ and ends at 236℃. At 396℃ the major breakdown of polymer starts and ends at 547℃, whereas the final degradation of the clinoptilolite is represented by a small peak from 548℃ to 703℃. Then, there is no change in the TGA profile up to 703ºC. In the case of the DTA and DTG graph, the height or depth of the peaks expresses reactivity intensity [27, 28].

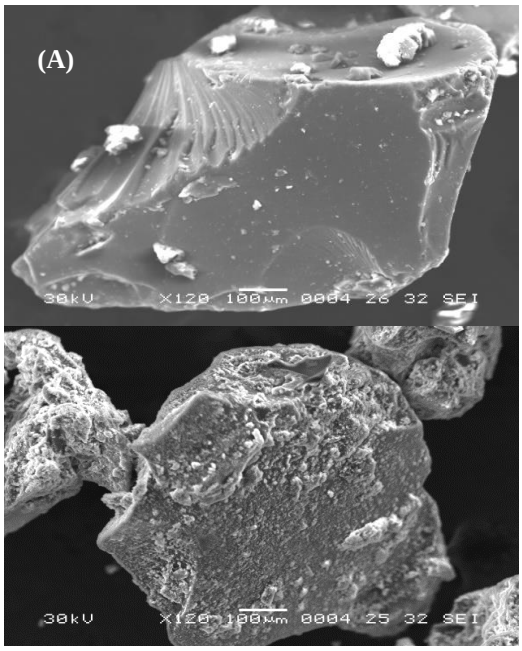

Figure 2: SEM micrographs of clinoptilolite(A) before and (B) after uranium adsorption

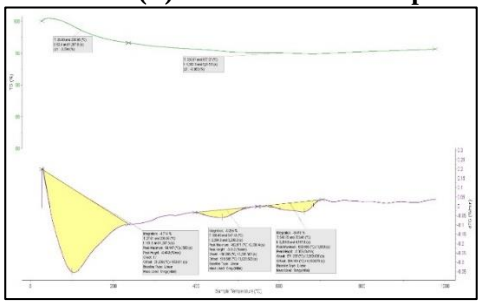

Figure (3): DTA-TGA of CH before heating treatment

3.2. Optimization of uranium adsorption conditions:

3.2.1. Effect of different media:

From these results, it is obvious that the nitric acid media is more suitable with an extraction efficiency of 36.8%. While the extraction efficiency of both hydrochloric acid and sulfuric acid media are 2.8% and 2.4% respectively when the natural clinoptilolite was used as represented in table (3).

Table (3): the Effect of different media on extraction efficiency

Type of acid media	Extraction efficiency %
HCl	2.8
H_2SO_4	2.4
HNO_3	36.8

3.2.2 Effect of natural clinoptilolite particle size

The particle size of natural clinoptilolite would make it amenable for extraction due to increasing the surface area of the extractant which is exposed to uranium in nitrate solution. The particle size of the natural clinoptilolite effect has been studied using samples having a size varying from –0.036, +0.036, +0.125, +0.25, and +0.5 mm. The obtained uranium extraction efficiencies are indicated in figure (4). From these results; it is obvious that uranium extraction efficiency decreases by increasing the natural clinoptilolite particle size. Where the extraction efficiency decreases (– 0.036 to +0.25 mm particle size) from 54.2% to 30.8% respectively and becomes at +0.5 mm particle size 33.4%.This behavior may be due to decreasing the surface area of the natural clinoptilolite as an extractant. So the particle size -36 mm for natural clinoptilolite was more sufficient for extraction of uranium with an extraction efficiency of 54.2%.

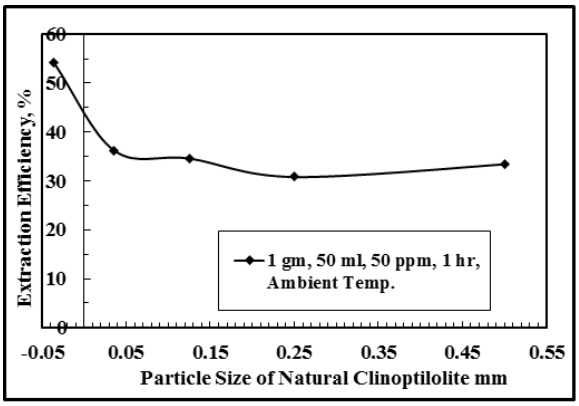

Figure (4): Effect of natural clinoptilolite particle size on uranium adsorption

3.2.3. Effect of Solution pH on the Extraction Efficiency

The effect of solution pH results on the extraction efficiency from the nitric acid medium using the hydrothermal treatment clinoptilolite was illustrated in Figure (5). From these results, it is clear that the extraction efficiency increased when the pH increased from 1.0to 2.5 with extraction efficiency 15.2 and 73.4 respectively. While by increasing the pH from 2.5 to 3.5 the extraction efficiency decreased to 26.0% respectively. Maximum extraction efficiency was achieved at pH 2.5 with an extraction efficiency of 73.4%.

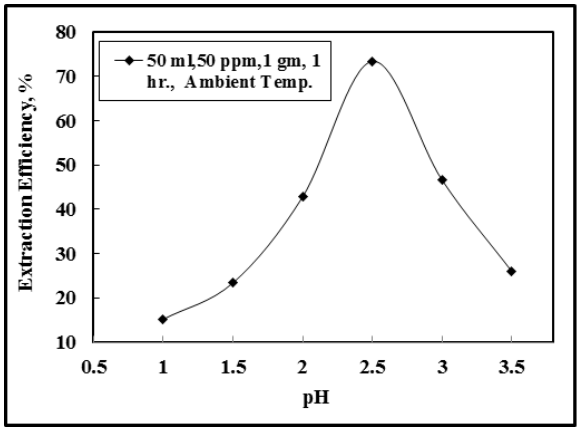

Figure (5): Effect of pH on uranium uptake using natural clinoptilolite

3.2.4. Effect of Initial Uranium Concentration:

Results of studying this factor using hydrothermal treatment clinoptilolite were illustrated in Figure (6). From these results, it is clear that uranium extraction efficiency was rabidly decreased from 78.4% to 24.8% when the initial concentration of uranium increased from 25 to 250 ppm respectively. This decreases my due to the low surface area of clinoptilolite which exposes to extraction consumed in high initial concentration of uranium.

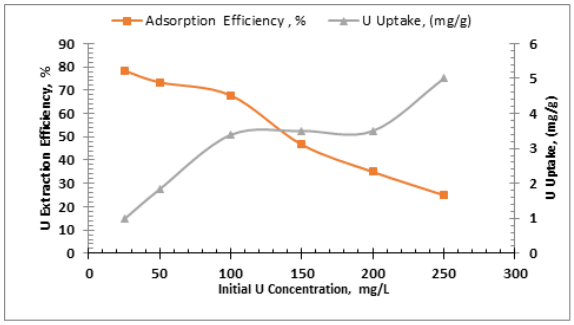

Figure (6): Effect of initial uranium concentration on uranium adsorption efficiency

3.2.5. Effect of contact time on the extraction efficiency:

The effect of the contact time upon the extraction efficiency was studied in the range of 5 to 120 min under the conditions of an aqueous solution of pH 2.5 containing 50ppm uranium at ambient temperature. Results of studying this factor were represented in figure (7). From these results, it is clear that the extraction efficiency was rapidly increased when the contact time increased from 5.0 min. (33.4%) to 50 min. (73.4%), and kept constant at 60 min. at extraction efficiency 73.4%. Then the extraction efficiency was slightly decreased when the contact time increased from 90 min. (70.6%) to 120 min. (66.8%). However, a contact time of 50 to 60 min. could be satisfied to attain the equilibrium between the phases during the extraction.

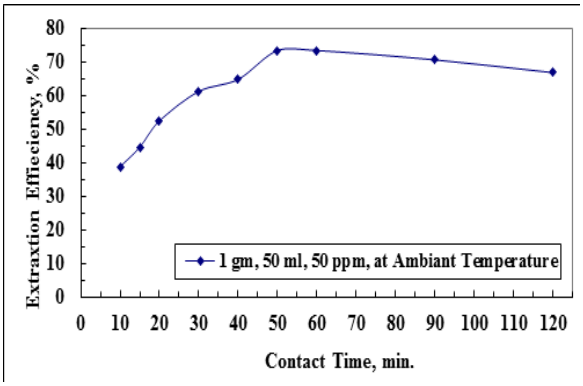

Figure (7): Effect of contact time on uranium adsorption efficiency

3.1.3 Effect of temperature:

The effect of temperature on the uranium uptake capacity of 1 g clinoptilolite from 50 ml solution assaying 50 mg/L was studied within the temperature range from 25 to 45 ºC at constant pH 2.5for60 minutes contact time. From the results represented in table (4), it is clear that the uranium uptake capacity decreased with increasing the temperature; therefore it was preferred to conduct the extraction at room temperature. The uranium uptake capacity at room temperature attained 18.75 mg/g while it decreased down to reach 13.0 mg/g at 45ºC. This decrease in the uranium uptake capacity with increasing the temperature might be due to decreasing the surface activity that leads to the decrease in the thickness of the boundary layer which increases the tendency of U to escape to the solution phase after extraction.

3.2 Sorption kinetics and mechanism:

The data obtained from batch experiments which were performed at different temperatures (25–45) ^{0}C were evaluated by using the simple Lagergrenequation[29] to determine the rate of the sorptive interactions assuming pseudo-first-order kinetics:

$$\log(q_e-q_t)=\log q_e-\left(\frac{k_1}{2.303}\right)t \qquad (4)$$

where q_t and q_e are the amounts of uranium adsorbed (mg/g) at the time, t (min), and equilibrium time (30 min), respectively an,d K_1 is the pseudo-first-order Lagergren adsorption rate constant (min $^{-1}$). The k_l values could be obtained by plotting log (qe – q_t) versus t for adsorption of uranium at different temperatures as shown in Figure 8. The values of the first-order rate constant (k_l) and correlation coefficient (R^2) obtained from these plots are listed in Table 4. The values of k_l indicate that the rate of the process increases with temperature. The first order mechanism suffered from inadequacies when applied to uranium sorption on the Clinoptilolite. One of the major discrepancies was observed when q_e values obtained from the pseudo-first-order plots were compared with the experimental q_e values are seen in Table 4. The experimental q_e values differed from the corresponding theoretical values. Thus, the interaction of uranium with the clinoptilolite does not follow the first-order kinetics

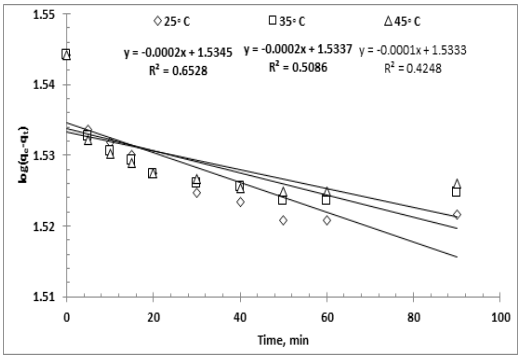

Figure 8: Lagergren plots for the adsorption of uranium

To ensure the description of the kinetics, the second-order kinetic equation was applied. The pseudo-second-order kinetics can be represented by the following linear equation [30]:

$$\frac{t}{q_t}=\frac{1}{K_2 q_e^2}+\left(\frac{1}{q_e}\right)t \qquad (5)$$

where k_2 is the second-order rate constant (g. mg^{-1} min^{-1}). The kinetic plots of t/q_t versus t for uranium are shown in Figure 9.

The plots show straight lines with good linearity temperatures. The calculated correlation coefficients are closer to unity for the pseudo-second-order kinetic model. The calculated equilibrium adsorption capacity (q_e) is consistent with the experimental data. The $k_2$values show the applicability of the above equation for the resin. Therefore the sorption reaction can be approximated more favorably by the pseudo-second-order sorption as the predominant mechanism.

Table (4): Effect of temperature on uranium uptake using clinoptilolite

Contact time, min.	Extraction Efficiency,%		
	Temp.25C°	Temp.35C°	Temp.45C°
5	33.4	36.2	37.8
10	38.8	42.8	43.8
15	44.6	47.2	48.2
20	52.4	52.8	52.4
30	61.2	57.0	55.2
40	64.8	58.6	58.8
50	73.2	64.4	60.6
60	73.2	64.4	60.6
90	70.6	61.2	57.0
120	66.8	56.8	52.4

Table 5: Data of kinetic parameters for uranium adsorption onto clinoptilolite

Temp, °C	Lagergreen pseudo first-order			pseudo second-order		
	K_1 (min $^{-1}$)	q_{ecal} (mg/ g)	R^2	K_2 (min $^{-1}$)	qe_{cal} (mg/ g)	R^2
25	0.00048	1.631	0.652	0.111	1.810	0.988
35	0.00035	1.621	0.508	0.376	1.639	0.996
45	0.00030	1.321	0.424	0.456	1.381	0.991

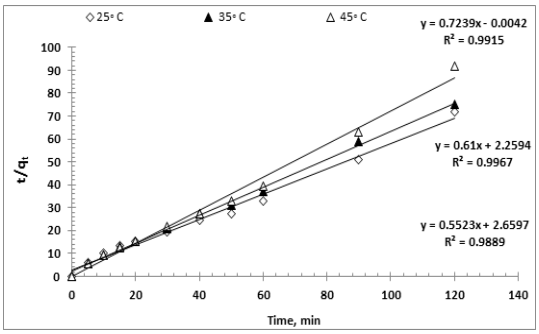

Figure 9: Pseudo second-order plots for the adsorption of uranium

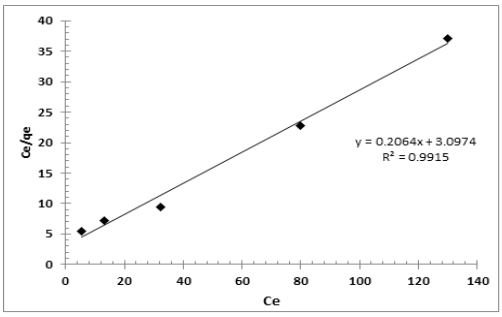

Figure 10: Langmuir isotherm plot for adsorption of uranium onto clinoptilolite

Adsorption Isotherm

Several common adsorption isotherm models were considered to fit the attained isotherm data under the equilibrium adsorption of the clinoptilolite. Examples of these models are Langmuir and Freundlich.

A- Langmuir Isotherm

Langmuir's model supposes that the adsorption occurs uniformly on the active sites of the sorbent, and once a sorbate occupies a site, no further sorption can take place at this site [30-31].

Thus, the Langmuir model is given by the following equation:

$$\frac{C_e}{q_e} = \frac{1}{bq_0} + \frac{C_e}{q_0} \qquad (6)$$

where: qo and b, the Langmuir constants, are the saturated monolayer sorption capacity and the sorption equilibrium constant, respectively. A plot of Ce/qe versus Ce would result in a straight line with a slope of 1/qo and an intercept of 1/bqo as seen in Figure 10. The Langmuir parameters are given in Table 6.

B- Freundlich Isotherm

The Freundlich model stipulates that the ratio of solute adsorbed to the solute concentration is a function of the solution. The empirical model was shown to be consistent with the exponential distribution of active centers, characteristic of heterogeneous surfaces. The amount of solute adsorbed at equilibrium, qe, is related to the concentration of solute in the solution, Ce, by the following:

$$q_e = K_F C_e^{1/n} \qquad (7)$$

This expression can be linearized to give:

$$\log q_e = \log K_F + \frac{1}{n}\log C_e \qquad (8)$$

where K_F and n are the Freundlich constants, which represent sorption capacity and sorption intensity, respectively. A plot of (logqe) versus (logCe) would result in a straight line with a slope of (1/n) and intercept of (log KF) as seen in Figure 11. Freundlich constants are given in Table 6.

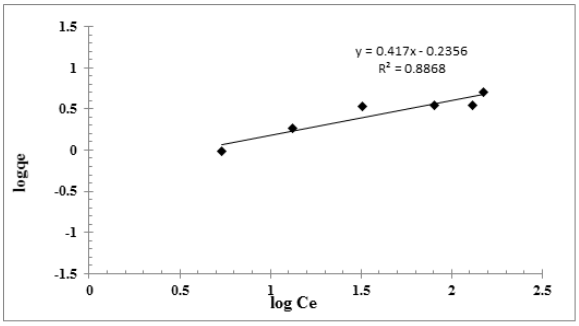

Figure 11: Freundlich isotherm plot for adsorption of uranium onto clinoptilolite

Comparing the isotherms applied with the experimental results, Freundlich gave the best fit, while Langmuir isotherms did not fit well.

Thermodynamic Characteristics

The thermodynamic parameters of the studied adsorption process have been determined for uranium adsorption upon clinoptilolite. A Series of experiments were carried out at various temperatures ranging from 25 to 58 ºC. These parameters were calculated for this system using the following Van't Hoff equation:

$$\log K_d = \frac{\Delta S}{2.303R} - \frac{\Delta H}{2.303RT} \qquad (9)$$

whereK_d (ml/g), ΔH (KJ/mol), ΔS (J/mol.K), T (Kelvin), and R (KJ/K.mol) are the distribution coefficient, the enthalpy, the entropy, the temperature in Kelvin, and the molar gas constant respectively. The plotting of log K_d against 1/T for uranium adsorption is shown in Figure 12.

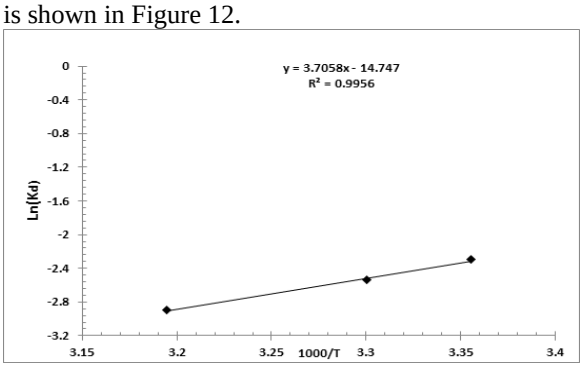

Figure 12: Plot of Ln Kd versus 1/T of uranium ions onto clinoptilolite

The values of ΔH and ΔS were obtained from the slope and intercept of the latter plot while the Gibbs free energy, ΔG (KJ/mol), is calculated from the following equation:

$$\Delta G = \Delta H - T\Delta S \qquad (10)$$

The calculated values of the thermodynamic parameters for U (VI) adsorption on clinoptilolite is given in Table 7. It was found that the enthalpy change (ΔH) and the entropy change (ΔG) were calculated to be -11.1948KJ/mol and 13.88318KJ/mol respectively. Thus, the adsorption process was found to be endothermic and non-spontaneous. The increased value of ΔS indicates a decrease in the randomness at the solid/solution interface during the sorption of the metal ion onto the sorbent.

4. Summary and conclusions

Natural clinoptilolite was characterized by scanning electron microscopy (SEM) and X-ray diffraction (XRD)Natural clinoptilolite has been used to remove uranium from an acidic solution. The batch tests which were performed to optimize the uranium adsorption by clinoptilolite indicate that 5 mg U/g clinoptilolite maximum saturation capacity was attained by adjusting the pHat2.5for 60 minutes contact time and with clinoptilolite to Liquor ratio of 1/250 at ambient temperature. By applyingLagergren equation, the sorption reaction can be approximated more favorably by the pseudo-second-order sorption as the predominate mechanism and the values of k_2"second-order rate constant" indicate that the rate of the process decreases with temperature.

Table 6: Langmuir and Freundlich isotherms parameters for uranium adsorption onto clinoptilolite

Langmuir model parameters			Freundlich model parameters		
q_o (mg/g)	b (L/mg)	R^2	n	K_f (mg/g)	R^2
4.84	0.066	0.991	1.72	2.39	0.886

Table 7: Thermodynamic data for sorption of uranium ions onto clinoptilolite

ΔH KJ/mol	ΔS J/mol.K	ΔG KJ/mol
-30.81	-0.1226	-5.7267

A Langmuir isotherm model is suitable for the description of the adsorption equilibrium of uranium onto clinoptilolite. From the thermodynamic parameters, a negative value of ΔH shows that uranium adsorption is exothermic and the negative ΔS parameter suggests decreasing the system randomness at the solid-liquid interface during the adsorption process.

References

1. Nassar, N.T., and Fortier, S.M., 2021, Methodology and technical input for the 2021 review and revision of the U.S. Critical Minerals List: U.S. Geological Survey Open-File Report 2021–1045, 31 p., https://doi.org/10.3133/ofr20211045.

2. Ambrozova, P.; Kynicky, J.; Urubek, T.; Nguyen, V.D. Synthesis and Modification of Clinoptilolite. Molecules 2017, 22, 1107. https://doi.org/10.3390/molecules22071107

3. Alberti, A. 1975. The crystal structure of two clinoptilolites. Tschermaks Mineral. Petrogr. Mitt. 22, 25-37

4. Baerlocher, C.; McCusker, L.B.; Olson, D.H. Atlas of Zeolite Framework Types, 6th ed.; Atlas of Zeolite Framework Types; Elsevier: Amsterdam, the Netherlands, 2007; ISBN 978-0-08-055434-1.

5. Zhen-Wu, B.Y., Prentice, D.P., Ryan, J.V. et al. zeo19: A thermodynamic database for assessing zeolite stability during the corrosion of nuclear waste immobilization glasses. npj Mater Degrad 4, 2 (2020). https://doi.org/10.1038/s41529-019-0106-1

6. Snellings R A, Gualtieri A F, Elsen J (2009) The Rietveld structure refinement of an exceptionally pure sample of clinoptilolite from Equador and its Na-, K-, and Ca- exchanged forms, ZeitschriftfürKristallographie Supplement, 30, 395-400

7. AlsenoK.MosaiHlangananiTutuSimultaneous sorption of rare earth elements (including scandium and yttrium) from aqueous solutions using zeolite clinoptilolite: A column

8. Minerals EngineeringVolume 161, 15 January 2021, 106740 10.1016/j.mineng.2020.106740

9. Bakatula, Elisée N., Mosai, Alseno K., & Tutu, Hlanganani. (2015). Removal of uranium from aqueous solutions using ammonium-modified zeolite. South African Journal of Chemistry, 68, 165-171. https://dx.doi.org/10.17159/0379-4350/2015/V68A23

10. Ahmadi M., Haghighi M., Kahforoushan D. Influence of active phase composition (mn, ni, mn*x*ni10−*x*) on catalytic properties and performance of clinoptilolite supported nanocatalysts synthesized using ultrasound energy toward abatement of toluene from polluted air. Process Saf. Environ. Prot. 2017; 106:294–308. DOI: 10.1016/j.psep.2016.06.029.

11. E. A. Haggag, A. A. Abdel-Samad, and A. M. Masoud, "Potentiality of Uranium Extraction from Acidic Leach Liquor by Polyacrylamide-Acrylic Acid Titanium Silicate Composite Adsorbent", International Journal of Environmental Analytical Chemistry, (2019), doi.org/10.1080/03067319.2019.1636037.

12. A. A. Abdel-Samad, M. M. Abdel Aal, E. A. Haggag, W. M. Yosef, Synthesis and Characterization of Functionalized Activated Carbon for Removal of Uranium and Iron from Phosphoric Acid, Journal of Basic and Environmental Sciences, 7 (2020) 140-153.

13. M. A. Mahmoud, E. A. Gawad, E.A. Hamoda and E. A. Haggag "Kinetics and Thermodynamic of Fe (III) Adsorption Type onto Activated Carbon from Biomass: Kinetics and Thermodynamics Studies", J. of Environmental Science, 11(4), (128-136), (2015).

14. JagodaDrozdzaka, Martine Leermakersa, YueGaoa, Marc Elskensa, VannaphaPhrommavanhb, Michael Descostesb, "Uranium aqueous speciation in the vicinity of the former uranium mining sites using the diffusive gradients in thin films and ultrafiltration techniques", Journal of Analytica Chimica Acta, Volume 913, 24 March 2016, Pages 94–103.

15. JunjieShena, b, Andrea Schäferb, c, "Removal of fluoride and uranium by nanofiltration and reverse osmosis: A review", Journal of Chemosphere, Volume 117, December 2014, Pages 679–691.

16. T. Sreenivas, K.C. Rajan, "Studies on the separation of dissolved uranium from alkaline carbonate leach slurries by resin-in-pulp process", Journal of Separation and Purification Technology, Volume 112, 10 July 2013, Pages 54–60.

17. C.S. Kedari, S.S. Pandit, P.M. Gandhi, "Separation by competitive transport of uranium(VI) and thorium(IV) nitrates across supported renewable liquid membrane containing trioctylphosphine oxide as metal carrier", Journal of Membrane Science 430 (2013) 188–195.

18. SawsanDacrory, El Sayed A. Haggag, Ahmed M. Masoud, Shaimaa M. Abdo, Ahmed A. Eliwa, and Samir Kamel. "Innovative Synthesis of Modified Cellulose Derivative as a Uranium Adsorbent from Carbonate Solutions of Radioactive Deposits, Journal of Cellulose, 29 May 2020. https://doi.org/10.1007/s10570-020-03272-w.

19. Zhaowu Zhu, Yoko Pranolo, Chu Yong Cheng, "Uranium recovery from strong acidic solutions by solvent extraction with Cyanex 923 and a modifier", Journal of Minerals Engineering, Volume 89, April 2016, Pages 77–83.

20. Y. M. Khawassek, A. A. Eliwa, E. A. Haggag, S. A. Mohamed and S. A. Omar "Equilibrium, Kinetic and Thermodynamics of Uranium Adsorption by Ambersep 400 SO4 Resin", Arab

Journal of Nuclear Sciences and Applications, Vol 50, 4, (100-112), (2017). Web site: esnsa-eg.com.

21. Qiang Song, Lijian Ma, Jun Liu, ChiyaoBai, JunxiaGeng, Hang Wang, Bo Li, Liyue Wang, Shoujian Li, "Preparation and adsorption performance of 5-azacytosine-functionalized hydrothermal carbon for selective solid-phase extraction of uranium", Journal of Colloid and Interface Science, Volume 386, Issue 1, 15 November 2012, Pages 291–299.
22. Reeder, R.J., Nugent, M., Tait, C.D., Morris, D.E., Heald, S.M., Beck, K.M., Lanzirotti, A., 2001. Co-precipitation of uranium (VI) with calcite: XAFS, micro-XAS, and luminescence characterization. Geochim. Cosmochim. Acta 65, 3491–3503.
23. Young Gun Ko, Jong-Myoung Lim, Geun-Sik Choi, Kun Ho Chung, MunJa Kang, "Characterizations of electrodeposited uranium layer on stainless steel disc", Journal of Colloids and Surfaces A: Physicochemical and Engineering Aspects, Volume 487, 20 December 2015, Pages 121–130.
24. Y. M. Khawassek, A. A. Eliwa, E. A. Haggag, S. A. Omar and S. A. Mohamed "Adsorption of rare earth elements by strong acid cation exchange resin thermodynamics, characteristics, and kinetics", SN Applied Sciences (2019) 1:51. doi.org/10.1007/s42452-018-0051-6
25. Z. Marczenko, M. Balcerzak "Preconcentration and Spectrophotometry in Inorganic Analysis. Elsevier Science BV, Amsterdam the Netherlands" (2000).
26. A. S. El-Sheikh, E. A. Haggag, and N. R. Abd El-Rahman" Adsorption of Uranium from Sulfate Medium Using a Synthetic Polymer; Kinetic Characteristics", Radiochemistry, 2020, Vol. 62, No. 4, pp. 499–510. doi.org 10.1134/S1066362220040074
27. R.R. Sheha," Sorption behavior of Zn(II) ions on synthesized hydroxyapatites", J. Colloid Interf. Sci. Volume 310 (2007) pp 18-26
28. Małecka, B., Łącz, A., Drożdż, E. MałeckiA.,"Thermal decomposition of d-metal nitrates supported on alumina". J Therm Anal Calorim 119, 1053–1061 (2015). https://doi.org/10.1007/s10973-014-4262-9
29. Hamza MF, Fouda A, Elwakeel KZ, Wei Y, Guibal E, Hamad NA. Phosphorylation of Guar Gum/Magnetite/Chitosan Nanocomposites for Uranium (VI) Sorption and Antibacterial Applications. Molecules. 2021 Mar 29;26(7):1920. DOI: 10.3390/molecules26071920.
30. Lagergren, S. (1898) Zur theorie der sogenannten adsorption geloster stoffe, Kungliga Svenska Vetenskapsakademiens. Handlingar, 24, 1-39.
31. Y.S. Ho, G. McKay, Pseudo-second order model for sorption processes", Process Biochem. 34 (1999) pp 451- 465.
32. Langmuir, The adsorption of gases on plane surfaces of glass, mica, and platinum, American Chemical Society, 40, 1918, 1361-1368.
33. H. Freundlich, Adsorption in solution, Physical and Chemical Society, 40, 1906, 1361-1368.